Nonlinear finite element analyses of reinforced concrete beam-column joints subjected to cyclic loading

Nonlinear finite element analyses of reinforced concrete beam-column joints subjected to cyclic loading

J Handoko[1], A Gunawan[1], J Chandra[1*], and H Wibowo[2]

[1] Civil Engineering Department, Petra Christian University, Jl. Siwalankerto 121-131, Surabaya, Indonesia
[2] Department of Civil, Construction, and Environmental Engineering, Iowa State University, 813 Bissell Road, Ames, Iowa, United States of America

[*] Corresponding author: chandra.jimmy@petra.ac.id

Abstract. Interaction of forces and moments in a beam-column joint is complex and most of the time nonlinear. Thus, a simple, global model is insufficient to estimate the performance and behavior of the joint. Results from several nonlinear finite element analyses of beam-column joints using VecTor2 are presented herein. Four interior and two exterior beam-column joint models with three different types of failure were studied. The analysis results in terms of force-drift ratio curves and crack patterns were then compared to the experimental results. In general, the results obtained from VecTor2 were satisfactory, but in some cases the program could not accurately capture the strength degradation observed in the specimen with joint shear failure. Moreover, the crack patterns were not accurately captured. Nevertheless, VecTor2 can still estimate the peak forces well for all specimens in this study.

1. Introduction

In reinforced concrete framing systems, beam-column joint connections play an important role in the global performance. Code provisions, therefore, provide specific requirements for these connections, especially if they are designed to accommodate seismic actions. Therefore, understanding the behavior of beam-column joints would lead to a better design. In this study, some numerical models were developed in VecTor2 computer software. The analysis results were then validated using the available experimental results from the literature. The objective of this study is to explore the capabilities and limitations of VecTor2 in terms of predicting the beam-column joint responses.

To complement any experimental study, typically numerical models are developed to predict the experimental results and further explore the parameters that cannot be included in the experimental program for various reasons. More robust numerical models can be developed and analyzed using finite element methods. Macro and micro finite element modeling can be used, depending on the level of details that need to be incorporated. Macro modeling is less detailed but has a faster computational time compared to micro modeling. Purnomo, Octaviani, Chiaulina, and Chandra [1] proposed a macro-lump plasticity model with the modified bond-slip model for several reinforced concrete (RC) beam-column joints. The model consisted of spring elements for defining the beam, column, joint, and bond-slip responses. From the research, it was found that the cyclic behavior of RC beam-column joints can be simulated well by the modified model. On the other hand, more fine tuning can be achieved with micro modeling, for example, the use of distributed plasticity and individual element-level constitutive relationship, which in turn lead to a more accurate model. Although micro modeling takes longer

computational time, recent developments in computer hardware have made it manageable, and is utilized in this study.

In this paper, nonlinear finite element analyses of interior and exterior beam-column joints subjected to cyclic loading using Version 4.4 of VecTor2 Basic [2] computer software are presented. VecTor2 is capable of analyzing two-dimensional reinforced concrete membrane structures. This software was developed based on the Modified Compression Field Theory (MCFT) by Vecchio and Collins [3] and Disturbed Stress Field Model (DSFM) by Vecchio [4]. VecTor2 has been demonstrated to produce good results in estimating the responses of reinforced concrete structures subjected to monotonic, cyclic, and reversed cyclic loading [5]. In this research, the focus is to investigate the capabilities of VecTor2 Basic Version in estimating the structural responses of beam-column joint models in terms of force-drift ratio curves and crack patterns.

2. Selected experimental tests from literature

All beam-column joints modeled in this research were chosen so they can be validated with results from experimental tests in the literature. The beam-column joint specimens presented herein consist of two interior joints tested by Li and Leong [6], one interior joint tested by Zhang and Li [7], one interior joint tested by Alaee and Li [8], one exterior joint tested by Alaee and Li [9], and one exterior joint tested by Hwang, Park, Choi, Chung, and Kim [10].

2.1. AS3 and NS3 specimens by Li and Leong [6]

These specimens were high-strength concrete interior beam-column joints subjected to constant column axial load and quasi-static horizontal cyclic load. The column axial load was equal to 2,470 kN. The horizontal loadings applied were equal to 0.50%, 1.00%, 1.50%, 2.00%, 2.50%, 3.00%, 3.50%, and 4.00% story drift. From the experiment, the AS3 specimen had cracks that mainly occurred on the beam and the reinforcement was found to yield and buckle at the end of the test. The AS3 specimen failed due to the flexural failure at the beam. On the other hand, beam flexural failure was observed to be the dominant failure mode for NS3 specimen. Furthermore, there was no serious joint core deterioration by the end of the test and the column remained at the elastic behavior. The elevation view of the specimen can be seen in Figure 1 and the material properties can be found in Table 1.

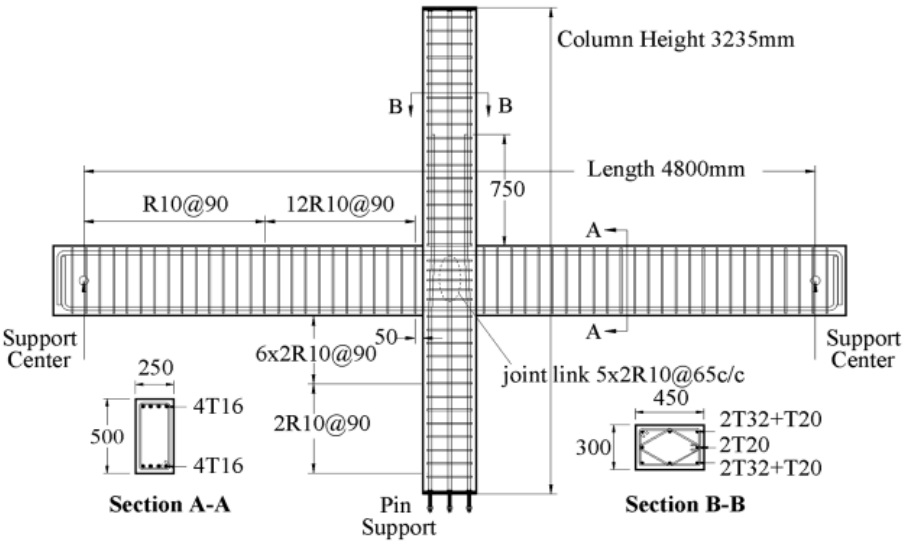

Figure 1. Details of AS3 and NS3 specimens [6]

2.2. IJ-U1 specimen by Zhang and Li [7]

Zhang and Li [7] tested eight full-scale specimens subjected to lateral cyclic loading to study the effect of rebar corrosion. The selected specimen for this study, specimen IJ-U1, was their control specimen without corroded transverse rebars. The axial load ratio was equal to 0.15. Moreover, the horizontal

loadings applied were equal to 0.50%, 1.00%, 1.50%, 2.00%, 2.50%, 3.00%, 3.50%, 4.00%, 4.50%, 5.00%, 5.50%, 6.00%, and 7.00% story drift. From the experiment, it was found that the failure mode of IJ-U1 specimen was joint shear with the formation of beam plastic hinge. The elevation view of the specimen can be seen in Figure 2 and the material properties can be found in Table 1.

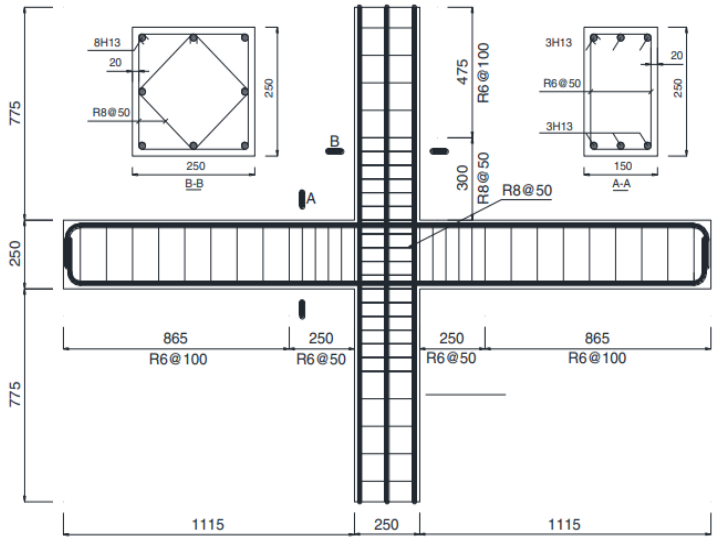

Figure 2. Details of IJ-U1 specimen [7]

2.3. IH80 specimen by Alaee and Li [8]

In this paper, Alaee and Li [8] reported experimental tests of high-strength concrete interior beam-column joints with high-yield-strength steel reinforcements. The specimens were subjected to a horizontal cyclic loading. The horizontal displacements correspond to story drift ratios of 0.50%, 0.75%, 1.00%, 1.50%, 2.00%, 2.50%, 3.00%, 3.50%, and 4.00%. The selected specimen for this study, specimen IH80, was not under constant compressive axial load. From the experiment, it was observed at the final loading stage that the concrete cover at the bottom corners of the beams-column interface were crushed. The details of the specimen can be seen in Figure 3. Furthermore, the material properties of the specimen can be found in Table 1.

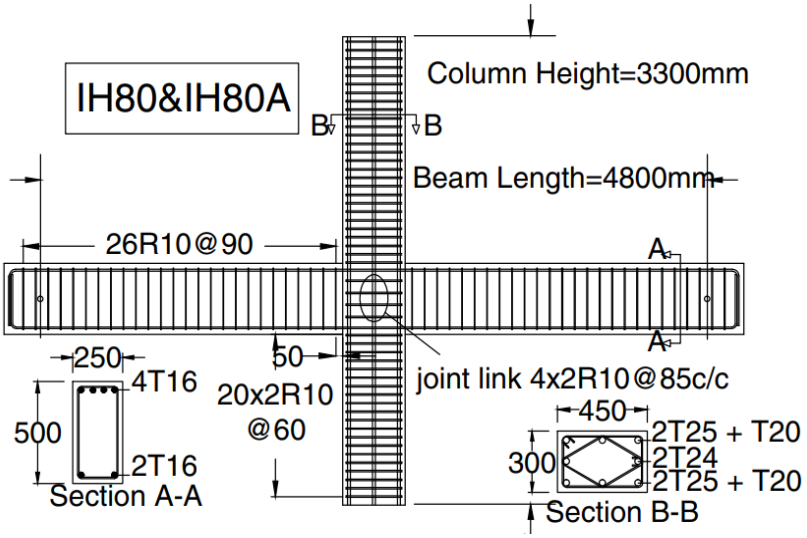

Figure 3. Details of IH80 specimen [8]

2.4. EH60A specimen by Alaee and Li [9]

Alaee and Li [9] tested five full-scale high-strength concrete exterior beam-column joints with high-yield-strength steel reinforcements to provide experimental evidence of their behavior when subjected to cyclic loading. The selected specimen for this study, specimen EH60A, was under a constant compressive axial load of $0.3f'_cA_g$. The horizontal loadings applied were equal to 0.50%, 0.75%, 1.00%, 1.50%, 2.00%, 2.50%, 3.00%, 3.50%, and 4.00% story drift. It was observed that this specimen displayed ductile failure mode with concrete crushing at beam ends and no noticeable joint crack. The elevation view of the specimen can be seen in Figure 4 and the material properties can be found in Table 1.

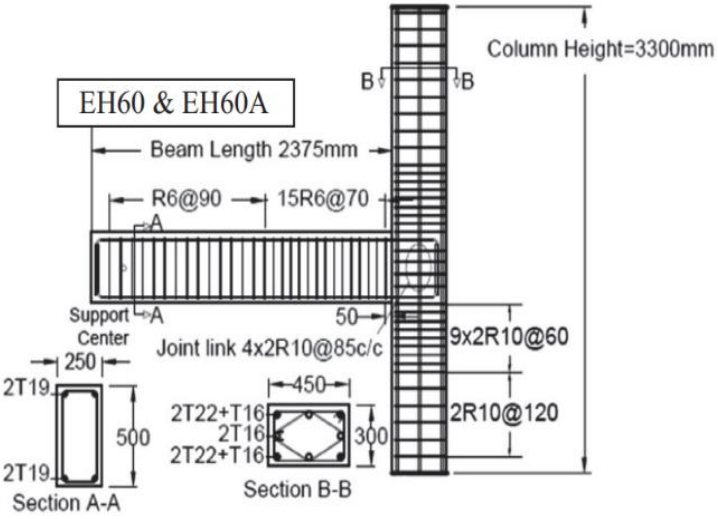

Figure 4. Details of EH60A specimen [9]

2.5. T1-400 specimen by Hwang, Park, Choi, Chung, and Kim [10]

Hwang, Park, Choi, Chung, and Kim [10] tested four interior and three exterior full-scale beam-column joint specimens with Grade 600 MPa longitudinal rebars under seismic loading. All the specimens tested were not under constant compressive axial load. The horizontal loadings applied were equal to 0.25%, 0.50%, 0.75%, and 1.00% story drift. After the story drift ratio of 1.00% was carried out, every subsequent drift ratio was increased by a 0.50% increment. From the experiment, it was found that the selected specimen for this study, specimen T1-400, failed due to the concrete crushing at the bottom side of the beam. The elevation view of the specimen can be seen in Figure 5 and the material properties can be found in Table 1.

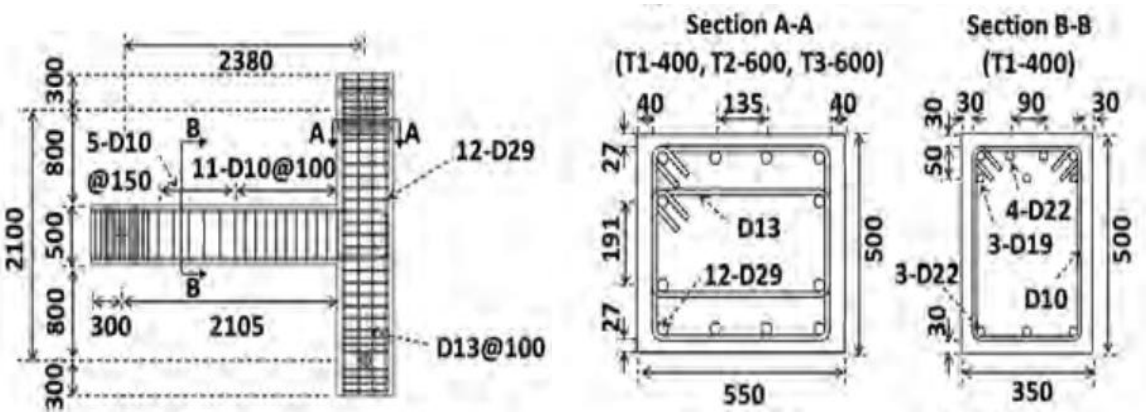

Figure 5. Details of T1-400 specimen [10]

Table 1. Material properties of beam-column joint specimens

Material properties	Specimens				
	AS3 & NS3	IJ-U1	IH80	EH80A	T1-400
Concrete, f'_c (MPa)	61.65	35.10	80.0	80.0	32.00
Young's Modulus, E_c (MPa)	36783.30	27845.27	42038.08	42038.08	26587.21
Beam					
Top Longitudinal Bars	4T16[a]	3H13[a]	4T16[a]	4T16[a]	4D22[b] 3D19[b]
f_y /f_u (MPa)	510/-	535/615	712/926	712/926	520/608 (D22[a]) 440/642(D19[a])
Bottom Longitudinal Bars	4T16[a]	3H13[a]	2T16[a]	2T16[a]	2D25[b]
f_y /f_u (MPa)	510/-	535/615	712/926	712/926	465/614
Stirrups	R10[c]-90	R6[c]-50 R6[c]-100	R10[c]-90	R10[c]-90	D10[b]-100
f_y /f_u (MPa)	357/-	380/583	-	563/650	-
Column					
Longitudinal Bars	4T32[a] 3T20[a]	8H13[a]	4T25[a] 2T24[a] 2T20[a]	4T22[a] 4T16[a]	12D29[b]
f_y /f_u (MPa)	510/-	535/615	719/929 (T25[a]) 506/651 (T24[a]) 711/914 (T20[a])	711/914 564/662	510/622
Stirrups	R10[c]-90	R8[c]-50 R6[c]-100	R10[c]-60 R10[c]-85	R10[c]-60 R10[c]-65	D13[b]-100
f_y /f_u (MPa)	357/-	300/430 (R8[c]) 380/583 (R6[c])	563/650	563/650	446/619

[a] T/H = High Tensile Steel Bars [b] D = Deformed Steel Bars [c] R = Plain Rounded Steel Bars

3. Nonlinear finite element modeling

The basic material models for concrete, reinforcement, and bond, provided by Version 4.4 of Vector2 Basic, were used in this study. The concrete material models used in defining the stress-strain curve of concrete in compression pre-peak and post-peak were the Hognestad Parabola [5] and Kent-Park [11], respectively. Furthermore, the Seckin with Bauschinger-Trilinear [5] model was used to define the stress-strain curve for the hysteretic response of the reinforcement. The bond properties can be defined with three points of bond stress and slip that were calculated with the Eligehausen [5] bond model. The stress-strain curves are shown in Figure 6 and Figure 7.

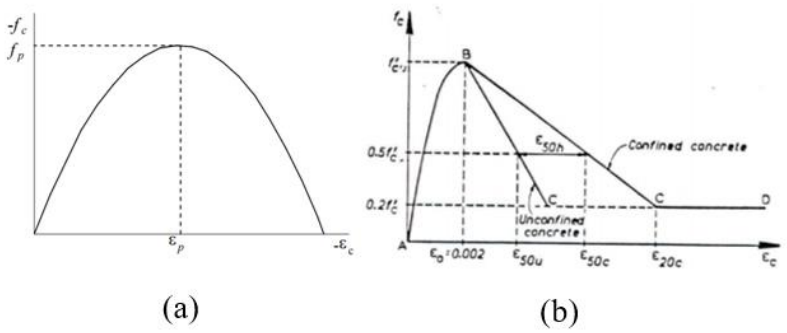

Figure 6. Stress-strain curves of concrete: (a) Hognestad Parabola [5], (b) Kent-Park [11]

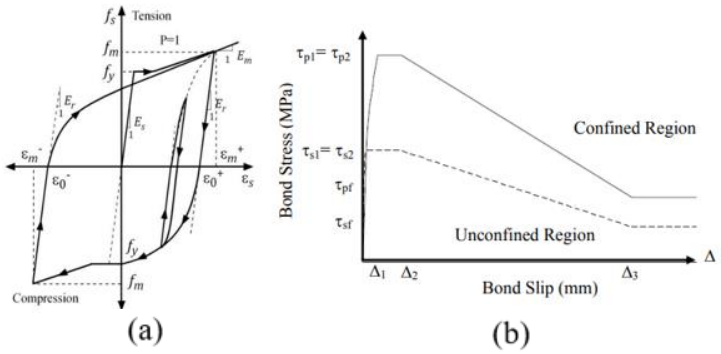

Figure 7. Stress-strain curve of reinforcement: (a) Seckin with Bauschinger-Trilinear [5] and bond-slip model (b) Eligehausen [5]

The specimens were modeled as two-dimensional structures. The concrete regions which consisted of unconfined, confined, and elastic regions were first defined. Elastic regions, located at the end of the beam and column, were modeled to avoid local failures. This was done due to the zero bending moment at the inflection points. The cracks observed in these regions were fewer than cracks in other regions. Furthermore, the reinforcement bars can be modeled as smeared or discrete. In this study, the longitudinal and in-plane transverse rebars were modeled as discrete truss elements. The out-of-plane transverse reinforcements were modeled as smeared. Linkage elements were also modeled to represent the bond behavior between the concrete and beam longitudinal rebars. On the other hand, the column longitudinal rebars were assumed to be perfectly bonded because in most cases, the column does not experience significant damage. The finite element modeling for interior and exterior beam-column joint specimens are shown in Figure 8.

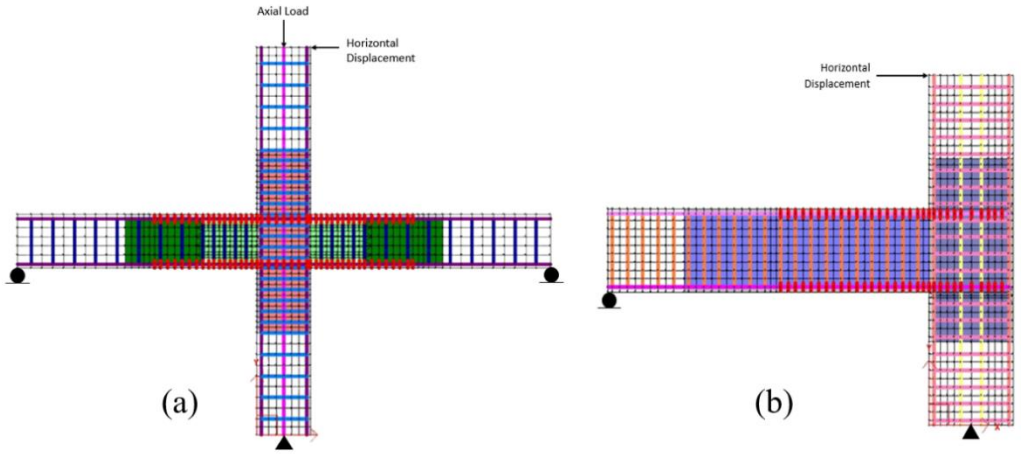

Figure 8. Typical VecTor2 modeling for (a) interior and (b) exterior beam-column joint specimens

4. Analysis results

The analysis results for the six specimens are presented in this section. The analysis results in terms of force-drift ratio curves and crack patterns were compared to the experimental results.

4.1. AS3 and NS3 specimen

From the experiment, it was found that the peak forces of AS3 specimen in the push and pull directions were 156.13 kN and 152.14 kN, respectively. On the other hand, the peak forces of NS3 specimen in the push and pull directions were 161.75 kN and 153.32 kN. From the nonlinear finite element analysis, it was found that the peak forces of AS3 specimen in the push and pull directions were 140.30 kN and

139.60 kN. The peak forces in the push and pull directions for NS3 specimen were 136.80 kN and 134.60 kN. The force-drift ratio curves of the specimens can be seen in Figure 9 and Figure 11. From the results, it can be seen that VecTor2 predicted lower peak forces as compared to the experimental results. Moreover, the strength degradation that occurred in the final loading stage of AS3 specimen could not be captured.

The reinforcement was observed to yield and buckle at the end of the test of AS3 specimen. This condition caused the concrete to spall mainly at the intersection of the beams and column. Moreover, the diagonal cracks slightly appeared on the joint. From the nonlinear finite element analysis, it was observed that the flexural cracks on the beam also appeared. On the other hand, flexural cracks on the beam top and bottom of NS3 specimen with limited joint diagonal cracks on the column were observed. The crack patterns of AS3 and NS3 specimens can be seen in Figure 10 and Figure 12.

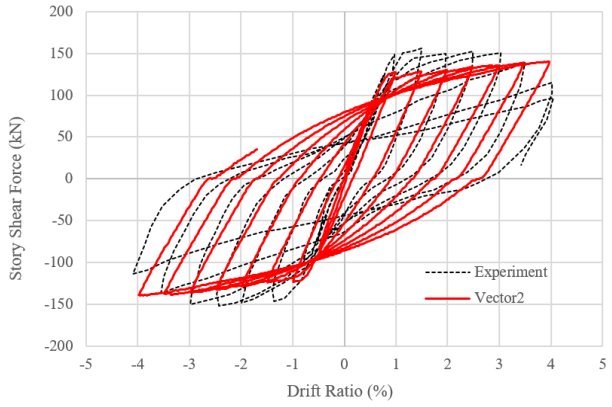

Figure 9. Force-drift ratio curve of AS3 specimen

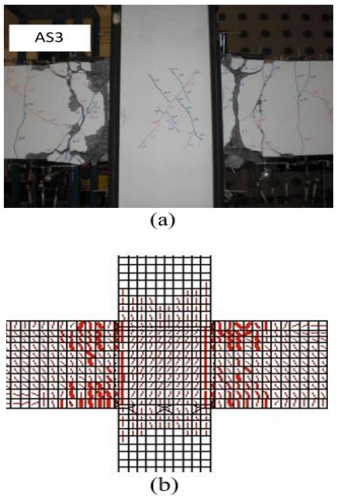

Figure 10. Cracking patterns of AS3 specimen obtained from: (a) experiment [6] and (b) VecTor2

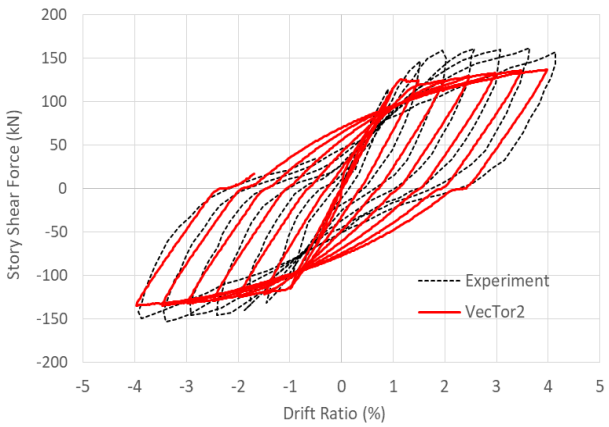

Figure 11. Force-drift ratio curve of NS3 specimen

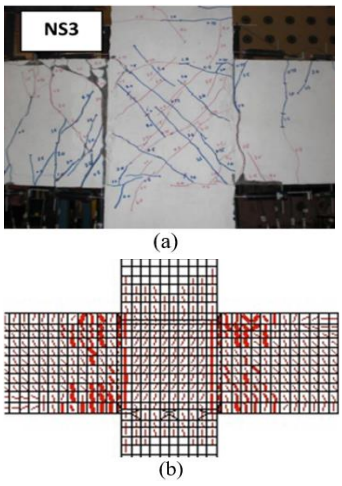

Figure 12. Cracking patterns of NS3 obtained from: (a) experiment [6] and (b) VecTor2

4.2. IJ-U1 specimen

From the experiment, it was found that the peak forces in the push and pull directions were 64.09 kN and 61.52 kN, respectively. In addition, it was reported that the specimen could sustain its maximum force capacity until 4.00% drift ratio. After 4.00% drift ratio, the strength degradation occurred. On the other hand, the analytical results of the peak forces in the push and pull directions were 61.30 kN and 60.20 kN. The force-drift ratio curve of the specimen can be seen in Figure 13. It can be seen that VecTor2 could give quite well predictions of the peak forces. However, the strength degradation captured was higher than the experimental results.

From the experiment, IJ-U1 specimen exhibited the formation of beam plastic hinge as the load increased. Diagonal cracks were observed on the joint section. Furthermore, bond deterioration occurred. From the nonlinear finite element analysis, the flexural cracks on the beam and diagonal cracks on the joint also appeared. The crack patterns of IJ-U1 specimen can be seen in Figure 14.

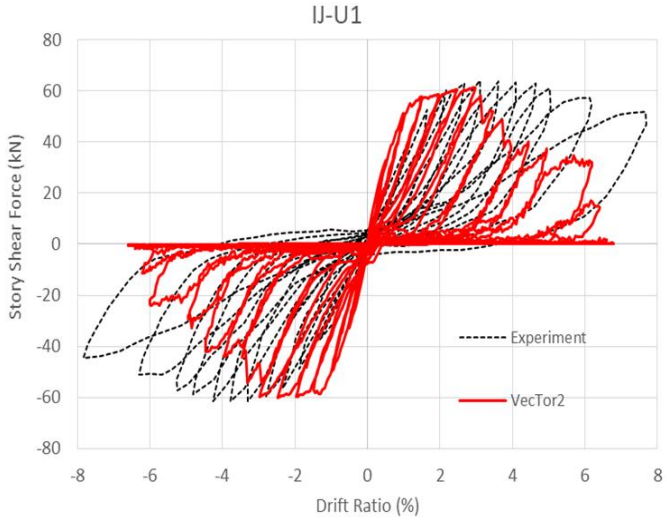

Figure 13. Force-drift ratio curve of IJ-U1 specimen

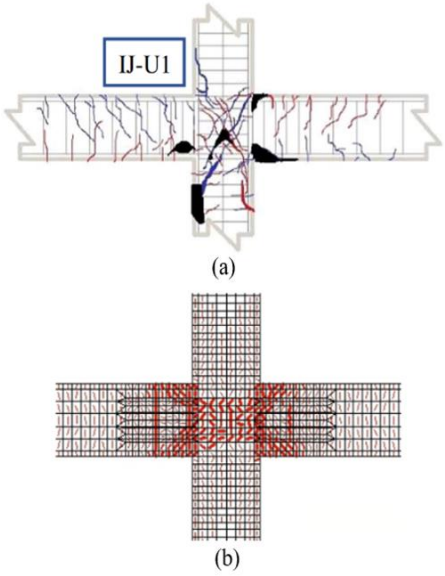

Figure 14. Cracking patterns of IJ-U1 specimen obtained from: (a) experiment [7] and (b) VecTor2

4.3. IH80 specimen

From the experiment, it was found that the peak forces of IH80 specimen in the push and pull directions were 147.19 kN and 151.61 kN, respectively. On the other hand, the analytical results of the peak forces in the push and pull directions were 145.80 kN and 144.60 kN. The force-drift ratio curve of the specimen can be seen in Figure 15. From the results, it can be seen that VecTor2 could predict the peak forces accurately. Moreover, the hysteretic behavior shown between the experimental and analytical results was also similar.

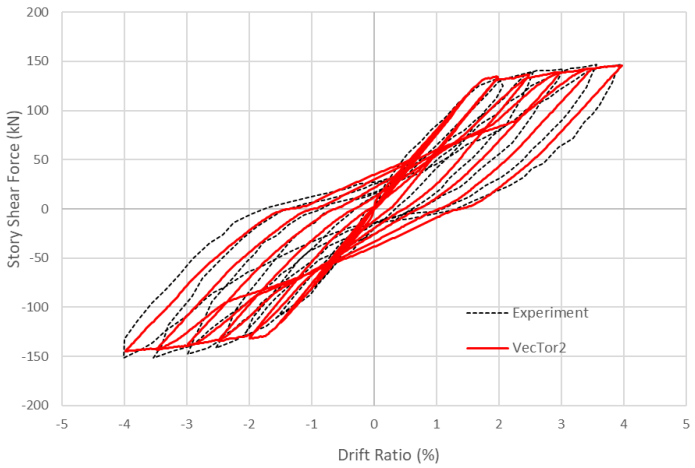

Figure 15. Force-drift ratio curve of IH80 specimen

Flexural cracks appeared on the top and bottom parts of the beam. Moreover, some diagonal cracks were observed on the joint. The concrete cover at the bottom corners of the beams-column interface were crushed. Slip of beam bars also occurred in the final loading stage. From the nonlinear finite element analysis, it was observed that the flexural cracks on the beam and joint diagonal cracks also appeared. The crack patterns of IH80 specimen can be seen in Figure 16.

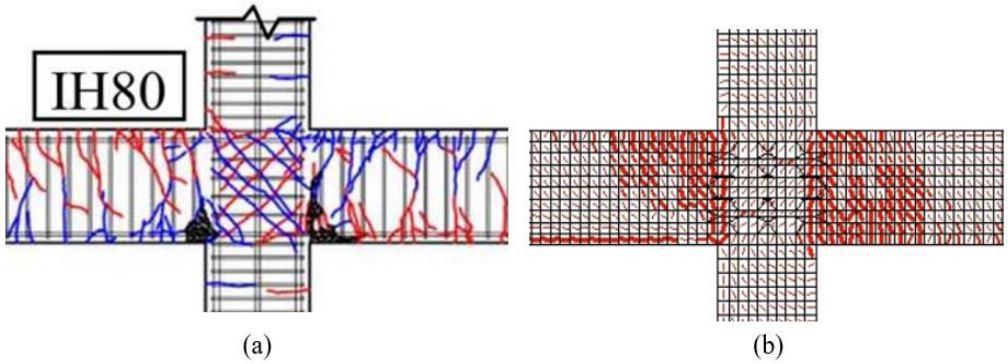

Figure 16. Cracking patterns of IH80 specimen obtained from: (a) experiment [8] and (b) VecTor2

4.4. EH60A specimen

From the experiment, it was found that the peak forces of EH60A specimen in the push and pull directions were 66.63 kN and 82.95 kN, respectively. The theoretical maximum force capacity, which was 69.00 kN, was exceeded. Furthermore, strength degradation did not occur because of the application of compressive axial load. From the nonlinear finite element analysis, it was found that the peak forces in the push and pull directions were 67.90 kN and 66.50 kN. The force-drift ratio curve of the specimen can be seen in Figure 17. Symmetrical hysteretic behavior in the push and pull directions was observed. However, the peak force in the pull direction was lower than the one from the experimental result.

EH60A specimen experienced beam flexural failure with no noticeable joint crack due to the application of compressive axial load. Moreover, the specimen experienced crushing of concrete at

beam ends. The flexural cracks on the beam-column interface and mild joint cracks could be captured by VecTor2. The crack patterns of EH60A specimen can be seen in Figure 18.

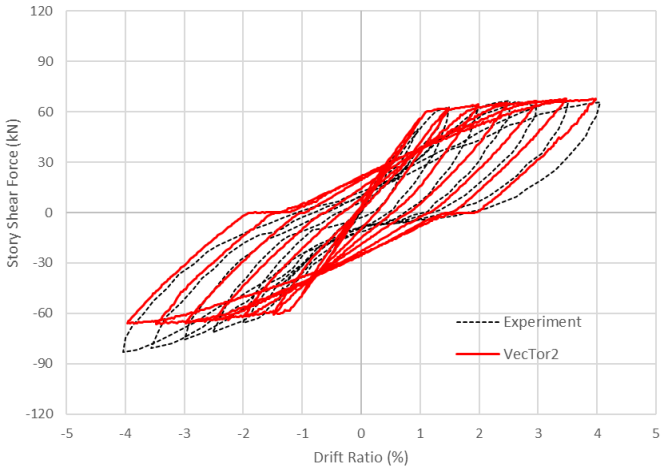

Figure 17. Force-drift ratio curve of EH60A specimen

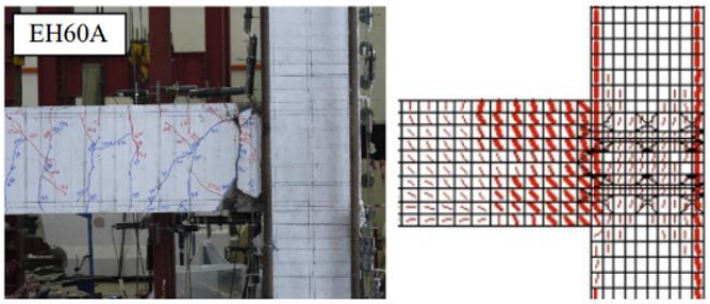

Figure 18. Cracking patterns of EH60A specimen obtained from: (a) experiment [9] and (b) VecTor2

4.5. T1-400 specimen

From the experiment, it was reported that the peak forces of T1-400 specimen in the push and pull directions were 260.39 kN and 157.70 kN, respectively. From the nonlinear finite element analysis, it was found that the peak forces in the push and pull directions were 291.80 kN and 158.00 kN. In addition, it was observed that the model could sustain its maximum force capacity until 4.00% drift ratio. On the other hand, the experimental result showed that the specimen failed in the pull direction after 3.00% drift ratio. The failure stage of the experimental specimen was shown by the sudden strength degradation at around 3.50% drift ratio. The force-drift ratio curve can be seen in Figure 19. From the analytical result, it can be seen that the prediction of the peak force in the push direction was higher than the one from the experimental result. Moreover, the strength degradation could not be well captured.

From the experiment, it was observed that T1-400 specimen experienced concrete crushing failure at the bottom side of the beam. From the nonlinear finite element analysis, it was observed that the crack majorly occurred at the intersection of the beam and column. The crack patterns of T1-400 specimen can be seen in Figure 20.

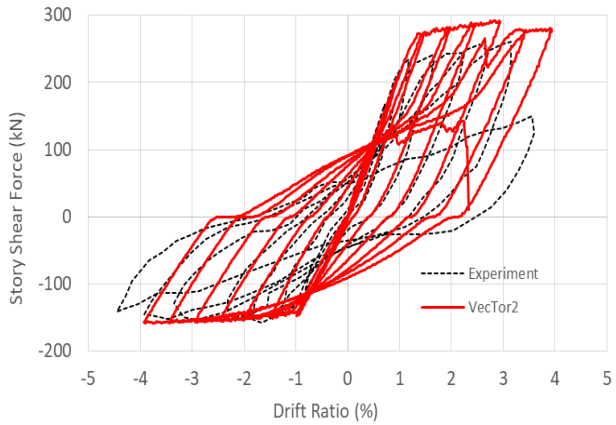

Figure 19. Force-drift ratio curve of T1-400 specimen

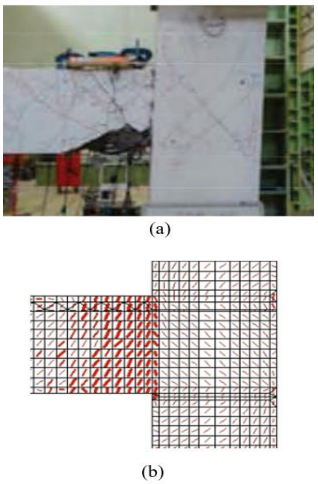

Figure 20. Cracking patterns of T1-400 specimen obtained from: (a) experiment [10] and (b) VecTor2

5. Summary of the analysis results

In general, good estimations of peak forces compared to the experimental results were shown by the VecTor2 analyses. The summary of the results can be seen in Table 2. Since the values of peak force ratios closed to 1.00, it can be concluded that a good agreement was shown between the experimental and analytical results.

Table 2. Summary of the analysis results

Specimen	Push/Pull	Peak force (kN)			Failure mode
		Experiment	VecTor2	Exp/VT2	
AS3	Push	156.13	140.30	1.11	Beam flexure
	Pull	152.14	139.60	1.09	
NS3	Push	161.75	136.80	1.18	Beam flexure
	Pull	153.32	134.60	1.14	
IJ-U1	Push	64.09	61.30	1.05	Joint shear
	Pull	61.52	60.20	1.02	
IH80	Push	147.19	145.80	1.01	Bond-slip
	Pull	151.61	144.60	1.05	
EH60A	Push	66.63	67.90	0.98	Beam flexure
	Pull	82.95	66.50	1.25	
T1-400	Push	260.39	291.80	0.89	Beam flexure
	Pull	157.70	158.00	1.00	

6. Concluding remarks

The peak forces in the push and pull directions for all the specimens modeled can be well predicted by VecTor2. However, the crack patterns were not accurately captured. Furthermore, the program could not accurately capture the strength degradation observed in the hysteretic behavior of the specimen with joint shear failure, such as IJ-U1 specimen. Nevertheless, VecTor2 can still give good estimations of the peak forces of this specimen.

References

[1] Purnomo J, Octaviani V, Chiaulina P K and Chandra J 2020 Evaluation of a macro lump plasticity model for reinforced concrete beam-column joint under cyclic loading *Civil Engineering Dimension* **22** 82-93
[2] Vecchio F J 2021 VecTor2 Basic [Computer software]. Retrieved from http://vectoranalysisgroup.com/software.html
[3] Vecchio F J and Collins M P 1986 The modified compression-field theory for reinforced concrete elements subjected to shear *ACI Journal* **83** 219-31
[4] Vecchio F J 2000 Disturbed stress field model for reinforced concrete: Formulation *J. Struct. Eng.* **126** 1070-77
[5] Wong P S, Vecchio F J and Trommels H *VecTor2 and FormWorks User's Manual 2nd Edition* (Toronto: University of Toronto)
[6] Li B and Leong C L 2015 Experimental and numerical investigations of the seismic behavior of high-strength concrete beam-column joints with column axial load *J. Struct. Eng.* **141** 04014220-1-14
[7] Zhang X and Li B 2022 Seismic performance of interior reinforced concrete beam-column joint with corroded reinforcement *J. Struct. Eng.* **148** 04021275-1-13
[8] Alaee P and Li B 2017 High-strength concrete interior beam-column joints with high-yield-strength steel reinforcements *J. Struct. Eng.* **143** 04017038-1-12
[9] Alaee P and Li B 2017 High-strength concrete exterior beam-column joints with high-yield strength steel reinforcements *Engineering Structures* **145** 305-21
[10] Hwang H J, Park H G, Choi W S, Chung L and Kim J K 2014 Cyclic loading test for beam-column connections with 600 MPa (87 ksi) beam flexural reinforcing bars *ACI Structural Journal* **111** 913-24
[11] Kent D C and Park R 1971 Flexural members with confined concrete *Journal of the Structural Division, Proceedings of the American Society of Civil Engineers* **97** 1969-90